Vibration analysis of symmetrically laminated thick rectangular plates using the higher-order theory and *p*-Ritz method

C. C. Chen
Department of Civil Engineering, The University of Queensland, Brisbane, Queensland 4072, Australia

K. M. Liew
Division of Engineering Mechanics, School of Mechanical and Production Engineering, Nanyang Technological University, Singapore 639798

C. W. Lim and S. Kitipornchai
Department of Civil Engineering, The University of Queensland, Brisbane, Queensland 4072, Australia

(Received 8 October 1996; accepted for publication 16 April 1997)

The free vibration analysis of symmetrically laminated thick rectangular plates is examined. The *p*-Ritz method is employed in which sets of uniquely defined polynomials are used as the admissible trial displacement and rotation functions. The energy integral expressions of the laminates are derived by incorporating the shear deformation using Reddy's higher-order plate theory [J. Appl. Mech. ASME **51**, 745–752 (1984)]. The formulation is basically applicable to rectangular laminates with any combination of free, simply supported, and clamped boundary conditions. To evaluate the validity and to demonstrate the applicability of the proposed method, a series of free vibration analyses of laminated composite plates is reported. Wherever possible, the accuracy of this analysis is validated through comparison with available results. Efforts are made to interpret the results to provide physical insight to the problem. © *1997 Acoustical Society of America.*
[S0001-4966(97)01708-6]

PACS numbers: 43.40.Dx [CBB]

INTRODUCTION

The unique properties of composite laminates, including high strength and high stiffness-to-weight ratios, high fatigue resistance, high damping, and potential for tailoring, have led to serious examination of their engineering performance in areas such as vibration, buckling, and stress analyses. An understanding of the vibration behavior of composite panels has particularly attracted many researchers to the possibility of furnishing an optimal design state. Numerous works have applied a direct extension of Kirchhoff's classical theory of plates to composite laminates. The assumptions underlying this theory, however, result in underestimation of deflection and overestimation of natural frequencies of a plate. Because of this disadvantage in the classical plate theory, numerous refined theories incorporating the transverse shear deformations have been proposed.

In existing literature, the first-order laminated plate theory was due to Yang *et al.*,[1] which was extended to the higher-order laminated plate theory by Reddy.[2] The first-order theory implies a conceptual paradox as the transverse shear strain does not vanish on the top and bottom surfaces. The thick laminated plate theories were developed to improve the modeling of transverse shear distribution. In addition, the higher-order theory discards the shear correction factors required in the first-order theory. A comprehensive review of the various refined plate theories for laminates proposed over the years has been summarized by Reddy and Robbins Jr.[3] and Noor and Burton.[4] Out of these theories, the theory used in the present study comes under the class of a single-layer displacement-based theory.[2] In this theory, the three-dimensional elasticity theory is reduced to two dimensions by replacing the laminated plate with an equivalent homogenous anisotropic plate and introducing a global displacement approximation in the thickness direction. The order of approximation is with respect to the distribution of displacements in the thickness direction. Thus, this theory provides reasonably accurate solutions in predicting the global behavior of composite laminates.

During the past decades, there has been much interest in the finite element method using various laminate plate theories because of its versatility.[5–7] However, sufficient numbers of discretized elements and nodes are required if there are curved boundary conditions. The *p*-Ritz method[8] somewhat improves these shortcomings by using the more traditional Rayleigh–Ritz method which assumes the entire plate as a single element and eliminates the need for discretization, mesh generation, and larger degrees of freedom. Excellent results were seen on earlier works for isotropic plates and thin and thick laminates.[9–12] An important feature of the Ritz method is the selection of admissible functions in the series representing the unknown functions in the displacement field. The accuracy and convergence of the solution are greatly dependent on the choice of the trial functions. In the present analysis, the *p*-Ritz functions are employed in which sets of uniquely defined polynomials are used as the admissible trial displacement and rotation functions. To account for the transverse shear effects, Reddy's higher-order shear deformation plate theory has been integrated with the *p*-Ritz method for solving the free vibration analysis of thick laminated plates with various boundary conditions.

It should be noted that Reddy and his associates[2,5] have presented results for only plates with opposite sides simply supported. Results for plates with general boundary conditions are still unavailable, to the authors' knowledge. Therefore, this paper attempts to provide examples of rectangular plates with various boundary conditions to show the applicability and versatility of the p-Ritz method, without the difficulty of mesh generation and continuity conditions of other discretization methods. Details of the analytical method and formulation for the problem of free vibration of laminated plates with combinations of clamped, simply supported, and free edges are presented. The accuracy and validity of the present method is established through convergence and comparison studies with the available literature results.

I. MATHEMATICAL FORMULATION

A. Preliminary

A thick, flat laminated plate with a thickness h, length a, width b, and composed of N orthotropic laminae oriented at angles θ is considered. The reference Cartesian coordinate system is located at the mid-plane of the laminated plate, as depicted in Fig. 1. The laminae are assumed to possess a plane of elastic symmetry parallel to the xy plane and be stacked symmetrically with respect to the middle surface of the laminated plate. The vibration frequencies of the symmetric laminates subjected to a variety of edge conditions, length-to-thickness ratios, aspect ratios, degrees of orthotropy, stacking angles, and numbers of layers are to be determined.

B. Energy expressions

By applying Reddy's higher-order shear deformation theory, the displacements of an arbitrary point of the thick laminated plate along the x, y, and z axes can be represented as

$$u(x,y,z,t)=u_0(x,y,t)+z\phi_x(x,y,t)-\frac{4z^3}{3h^2}\left(\phi_x(x,y,t)+\frac{\partial w(x,y,t)}{\partial x}\right), \tag{1a}$$

$$v(x,y,z,t)=v_0(x,y,t)+z\phi_y(x,y,t)-\frac{4z^3}{3h^2}\left(\phi_y(x,y,t)+\frac{\partial w(x,y,t)}{\partial y}\right), \tag{1b}$$

$$w(x,y,z,t)=w_0(x,y,t), \tag{1c}$$

where (u_0,v_0,w_0) are the displacement components of the mid-plane along the x, y, and z directions, respectively. The rotations about the x and y directions, respectively, are ϕ_x and ϕ_y.

Assuming transverse inextensibility, the strain–displacement relationship for any lamina in the Cartesian system can be expressed as

$$\varepsilon=L\mathbf{u} \tag{2}$$

with

$$\mathbf{u}=[u_0 \quad v_0 \quad w_0 \quad \phi_x \quad \phi_y]^T, \tag{3a}$$

$$\varepsilon=[\varepsilon_x \quad \varepsilon_y \quad \gamma_{yz} \quad \gamma_{xz} \quad \gamma_{xy}]^T, \tag{3b}$$

and

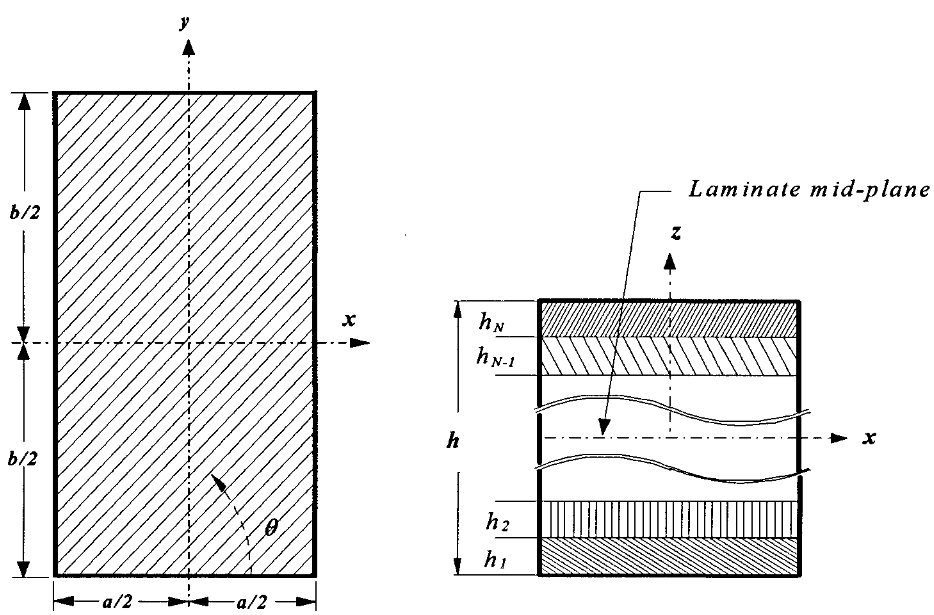

FIG. 1. Geometry of the laminated plate.

$$
L=\begin{bmatrix}
\frac{\partial}{\partial x} & 0 & -\frac{4z^3\partial^2}{3h^2\ \partial x^2} & \left(z-\frac{4z^3}{3h^2}\right)\frac{\partial}{\partial x} & 0 \\
0 & \frac{\partial}{\partial y} & -\frac{4z^3\partial^2}{3h^2\ \partial y^2} & 0 & \left(z-\frac{4z^3}{3h^2}\right)\frac{\partial}{\partial y} \\
0 & 0 & \left(1-\frac{4z^2}{h^2}\right)\frac{\partial}{\partial y} & 0 & \left(1-\frac{4z^2}{h^2}\right) \\
0 & 0 & \left(1-\frac{4z^2}{h^2}\right)\frac{\partial}{\partial x} & \left(1-\frac{4z^2}{h^2}\right) & 0 \\
\frac{\partial}{\partial y} & \frac{\partial}{\partial x} & -\frac{8z^3\partial^2}{3h^2\ \partial x\ \partial y} & \left(z-\frac{4z^3}{3h^2}\right)\frac{\partial}{\partial y} & \left(z-\frac{4z^3}{3h^2}\right)\frac{\partial}{\partial x}
\end{bmatrix}, \tag{3c}
$$

and the constitutive equations for the kth lamina are

$$\sigma_k=\mathbf{D}_k\varepsilon_k. \tag{4}$$

in which $\sigma_k=[\sigma_x\ \sigma_y\ \sigma_{yz}\ \sigma_{xz}\ \sigma_{xy}]^T$ and the stiffness matrix is defined by

$$
\mathbf{D}_k=\begin{bmatrix}
\overline{Q_{11}} & \overline{Q_{12}} & 0 & 0 & \overline{Q_{16}} \\
\overline{Q_{12}} & \overline{Q_{22}} & 0 & 0 & \overline{Q_{26}} \\
0 & 0 & \overline{Q_{44}} & \overline{Q_{45}} & 0 \\
0 & 0 & \overline{Q_{45}} & \overline{Q_{55}} & 0 \\
\overline{Q_{16}} & \overline{Q_{26}} & 0 & 0 & \overline{Q_{66}}
\end{bmatrix}_k . \tag{5}
$$

Here, $(\overline{Q_{ij}})_k$ are obtained by transforming the stacking angle θ and the stiffness constants $(Q_{ij})_k$ which are related to the material properties, E_1, E_2, ν_{12}, ν_{21}, G_{12}, G_{13}, G_{23}, of each ply. In terms of these engineering constants, $(Q_{ij})_k$ can be written in the form of

$$(Q_{11})_k=E_1/(1-\nu_{12}\nu_{21}), \tag{6a}$$

$$(Q_{12})_k=\nu_{12}E_2/(1-\nu_{12}\nu_{21}), \tag{6b}$$

$$(Q_{22})_k=E_2/(1-\nu_{12}\nu_{21}), \tag{6c}$$

$$(Q_{44})_k=G_{23}, \tag{6d}$$

$$(Q_{55})_k=G_{13}, \tag{6e}$$

$$(Q_{66})_k=G_{12}. \tag{6f}$$

In linear elasticity analysis, the strain energy for each ply is given by

$$U_k=\frac{1}{2}\int_{\mathscr{V}_k}\varepsilon_k^T\sigma_k\, dV_k, \tag{7}$$

where U_k and V_k are respectively the strain energy and the volume of the kth lamina. Hence, the total strain energy for the entire laminated plate is

$$U=\frac{1}{2}\sum_{k=1}^{N}\int\int_A\int_{h_{k-1}}^{h_k}(\sigma_x\varepsilon_x+\sigma_y\varepsilon_y+\sigma_{xz}\varepsilon_{xz}+\sigma_{yz}\varepsilon_{yz} + \sigma_{xy}\varepsilon_{xy})_k\ dz\ dA. \tag{8}$$

Accordingly, the total kinetic energy T associated with the vibration of laminated plate is

$$T=\frac{h}{2}\sum_{k=1}^{N}\int\int_A\rho_k\left[\left(\frac{\partial u}{\partial t}\right)^2+\left(\frac{\partial v}{\partial t}\right)^2+\left(\frac{\partial w}{\partial t}\right)^2\right]dA \tag{9}$$

in which ρ_k is the mass density per volume for the kth lamina.

The equivalent modulus for a multidirectional lamina is introduced:

$$(A_{ij},B_{ij},D_{ij},E_{ij},F_{ij},H_{ij}) =\sum_{k=1}^{N}\int_{h_k}^{h_{k+1}}\overline{Q_{ij}}(1,z,z^2,z^3,z^4,z^6)dz, \tag{10}$$

where all B_{ij} and E_{ij} vanish if laminates are stacked symmetrically about the mid-plane. The total potential energy U and total kinetic energy T can be further expanded in terms of the equivalent modulus (see the Appendix). The deflection and rotation functions of the laminate mid-plane are periodic in time. Therefore, for small amplitude vibration, we can assume that

$$u_0(x,y,t)=U(x,y)\sin\ \omega t, \tag{11a}$$

$$v_0(x,y,t)=V(x,y)\sin\ \omega t, \tag{11b}$$

$$w_0(x,y,t)=W(x,y)\sin\ \omega t, \tag{11c}$$

$$\phi_x(x,y,t)=\Theta_u(x,y)\sin\ \omega t, \tag{11d}$$

$$\phi_y(x,y,t)=\Theta_v(x,y)\sin\ \omega t. \tag{11e}$$

By substituting Eqs. (11a)–(11e) into the total potential energy U and the total kinetic energy T, we can obtain the maximum strain energy $U_{\max}$ and the maximum kinetic energy $T_{\max}$. The total energy functional Π of the plate is defined in terms of $U_{\max}$ and $T_{\max}$ as

$$\Pi=U_{\max}-T_{\max}, \tag{12}$$

which can be minimized using the p-Ritz method to obtain the vibration frequencies.

C. *p*-Ritz method

The displacement and rotation components, $U(x,y)$, $V(x,y)$, $W(x,y)$, $\Theta_u(x,y)$, and $\Theta_v(x,y)$, can be further simplified by using the nondimensional expressions

TABLE I. Notations for boundary conditions.

Boundary constraints[a]		$u_n=u_s=0$	$N_n=u_s=0$	$N_{ns}=u_n=0$	$N_{ns}=N_n=0$
Free	$\partial M_{ns}/\partial s+Q_n=0$ $M_n=0$	F_1	F_2	F_3	F_4
Simply supported	$w=0$ $M_n=0$	S_1	S_2	S_3	S_4
Clamped	$w=0$ $\partial w/\partial n=0$	C_1	C_2	C_3	C_4

[a]Here, n and s indicate the directions normal and tangential to the corresponding supporting edges.

$$\xi=\frac{x}{a},\tag{13a}$$

$$\eta=\frac{y}{b}.\tag{13b}$$

Accordingly, the in-plane deflection and rotation functions can be expressed in the nondimensional $\xi\eta$ plane, leading to

$$U(\xi,\eta)=\sum_{i=1}^{m} c_i^u\varphi_i^u(\xi,\eta),\tag{14a}$$

$$V(\xi,\eta)=\sum_{i=1}^{m} c_i^v\varphi_i^v(\xi,\eta),\tag{14b}$$

$$W(\xi,\eta)=\sum_{i=1}^{m} c_i^w\varphi_i^w(\xi,\eta),\tag{14c}$$

$$\Theta_u(\xi,\eta)=\sum_{i=1}^{m} c_i^{\theta_u}\varphi_i^{\theta_u}(\xi,\eta),\tag{14d}$$

$$\Theta_v(\xi,\eta)=\sum_{i=1}^{m} c_i^{\theta_v}\varphi_i^{\theta_v}(\xi,\eta),\tag{14e}$$

where φ_i^u, φ_i^v, φ_i^w, $\varphi_i^{\theta_u}$, $\varphi_i^{\theta_v}$ are the so-called p-Ritz functions which are products of two-dimensional polynomials and basic functions. The associated c_i^u, c_i^v, c_i^w, $c_i^{\theta_u}$, $c_i^{\theta_v}$ are the unknown coefficients. The number of terms m in the series (14a)–(14e) can be obtained by

$$m=\frac{(p+1)(p+2)}{2},\tag{15}$$

where p is the degree of the set of two-dimensional polynomials.

The p-Ritz shape functions can be generated by assuming that

$$\varphi_i^\alpha(\xi,\eta)=\sum_{q=0}^{p}\sum_{j=0}^{q}\xi^{q-j}\eta^j\varphi_b^\alpha(\xi,\eta)\tag{16}$$

in which $\alpha=u,v,w,\theta_u,\theta_v$, and $\varphi_b^\alpha(\xi,\eta)$ denotes the basic function which must at least satisfy the geometric boundary conditions of the laminated plate. The basic function for the laminated plate can be expressed as

$$\varphi_b^\alpha=\prod_{s=1}^{4}[\Gamma_s(\xi,\eta)]^{\Omega_s^\alpha},\tag{17}$$

where $\Gamma_s(\xi,\eta)$ is the boundary equation of the sth supporting edge and Ω_s^α denotes the associated basic power. The basic functions consist of products of boundary expressions of the laminated plate raised to their associated basic powers to guarantee automatic satisfaction of geometric boundary conditions. Whitney[13] suggested that one member of each pair of the following four quantities must be prescribed along the boundary to ensure unique solutions to the governing equations

$$u_n;N_n \quad u_s;N_{ns} \quad \frac{\partial w}{\partial n};M_n \quad w;\ \frac{\partial M_{ns}}{\partial s}+Q_n.\tag{18}$$

TABLE II. Powers of basic functions for various combinations of boundary conditions.

Edge s	Power Ω_s^a 1					2					3					4				
α	u	v	w	θ_u	θ_v	u	v	w	θ_u	θ_v	u	v	w	θ_u	θ_v	u	v	w	θ_u	θ_v
$S_2F_4S_2F_4$	0	1	1	0	1	0	0	0	0	0	0	1	1	0	1	0	0	0	0	0
$C_1F_4C_1F_4$	1	1	2	1	1	0	0	0	0	0	1	1	2	1	1	0	0	0	0	0
$C_1F_2F_2F_2$	1	1	2	1	1	1	0	0	0	0	0	1	0	0	0	1	0	0	0	0
$C_2F_2F_2F_2$	0	1	2	0	1	1	0	0	0	0	0	1	0	0	0	1	0	0	0	0
$S_2S_2S_2S_2$	0	1	1	0	1	1	0	1	1	0	0	1	1	0	1	1	0	1	1	0
$S_3S_3S_3S_3$	1	0	1	0	1	0	1	1	1	0	1	0	1	0	1	0	1	1	1	0
$C_2S_2S_2S_2$	0	1	2	0	1	1	0	1	1	0	0	1	1	0	1	1	0	1	1	0
$S_2C_1S_2C_1$	0	1	1	0	1	1	1	2	1	1	0	1	1	0	1	1	1	2	1	1
$C_1C_1C_1C_1$	1	1	2	1	1	1	1	2	1	1	1	1	2	1	1	1	1	2	1	1
$C_2C_2C_2C_2$	0	1	2	0	1	1	0	2	1	0	0	1	2	0	1	1	0	2	1	0
$C_3C_3C_3C_3$	1	0	2	1	0	0	1	2	0	1	1	0	2	1	0	0	1	2	0	1

TABLE III. Convergence study of frequency parameters, $\lambda' = \omega h \sqrt{\rho/G}$, for an isotropic thick plate with different degree of polynomial (p).

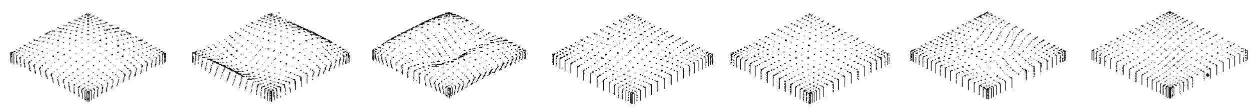

p	Mode shapes						
7	0.0930	0.2220	0.3407	0.4152	0.5256	0.6975	0.7510
9	0.0930	0.2220	0.3406	0.4151	0.5209	0.6846	0.7463
11	0.0930	0.2220	0.3406	0.4151	0.5208	0.6840	0.7454
13	0.0930	0.2220	0.3406	0.4151	0.5208	0.6840	0.7454
15	0.0930	0.2220	0.3406	0.4151	0.5208	0.6840	0.7454
CLPT	0.0963	0.2408	0.3853	0.4816	0.6261	0.8686	0.9632
Mindlin[16]	0.0930	0.2218	0.3402	0.4144	0.5197	0.6821	0.7431
Mallikarjuna[6,a]	0.0929	0.2216	0.3379	0.4184	0.5152	0.6941	0.7610
Noor[17]	0.0932	0.2226	0.3421	0.4171	0.5239	0.6889	0.7511

[a]Higher-order shear deformation theory.

Therefore, many types of boundary conditions are considered along the geometric and natural boundary constraints given in Eq. (18) and summarized in Table I. For examples, there are four types of simply supported conditions: S_1, S_2, S_3, and S_4. These supports have the transverse direction w constrained and varying in-plane support conditions. The most common simply supported condition is S_1 where both the normal and tangential displacements in the midplane are constrained. Another condition having physical interpretation is S_2 with transverse (w) and tangential (u_s) directions constrained which occur mostly in composite plates and sometimes termed ''freely supported.''[14,15] The basic powers Ω_s^α are assigned 0, 1, or 2 depending on whether the normal, tangential, or transverse direction is constrained at the edge. Details of basic power for various combinations of boundary conditions are listed in Table II. As shown in Fig. 1, $s=1$ refers to the edge at $x=-a/2$, and $s=2,3,4$ correspond to the subsequent edges, going counterclockwise. In detail, the nondimensional basic functions for the rectangular laminated plate are

$$\varphi_b^\alpha = (\xi-0.5)^{\Omega_1^\alpha}(\eta-0.5)^{\Omega_2^\alpha}(\xi+0.5)^{\Omega_3^\alpha}(\eta+0.5)^{\Omega_4^\alpha} \tag{19}$$

with $\alpha = u, v, w, \theta_u$, and θ_v.

By applying the Ritz method, we minimize the total energy functional Π with respect to the unknown coefficients,

$$\frac{\partial \Pi}{\partial c_i^u} = 0, \tag{20a}$$

$$\frac{\partial \Pi}{\partial c_i^v} = 0, \tag{20b}$$

$$\frac{\partial \Pi}{\partial c_i^w} = 0, \tag{20c}$$

$$\frac{\partial \Pi}{\partial c_i^{\theta_u}} = 0, \tag{20d}$$

$$\frac{\partial \Pi}{\partial c_i^{\theta_v}} = 0, \tag{20e}$$

for i from 1 to m. The differentiation leads to an eigenvalue equation,

$$\{\mathbf{K} - \lambda \mathbf{M}\}\{\mathbf{c}\} = \mathbf{0}, \tag{21}$$

where $\{\mathbf{c}\} = \{c^u \quad c^v \quad c^w \quad ac^{\theta_u} \quad bc^{\theta_v}\}^T$, and λ is the nondimensional eigenvalue defined as

$$\lambda = \frac{\omega ab}{h}\sqrt{\frac{\rho}{D_0}}, \tag{22}$$

with $D_0 = Q_{11}/12$. Details of the stiffness matrices **K** and the mass matrices **M** are shown in the Appendix.

TABLE IV. Convergence study of frequency parameters, $\lambda' = \omega h \sqrt{\rho/E_2}$, for a three-ply square laminate with different degree of polynomial (p).

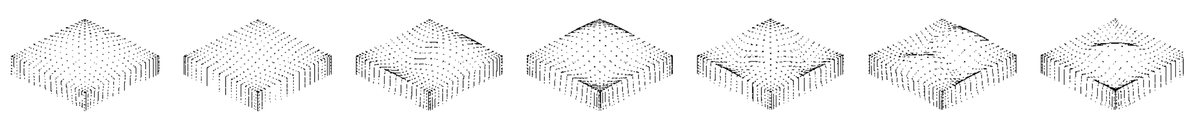

p	Mode shapes						
7	0.4537	0.6883	0.7322	0.8449	1.0182	1.1807	1.2653
9	0.4528	0.6883	0.7320	0.8442	1.0173	1.1801	1.2634
11	0.4523	0.6883	0.7320	0.8438	1.0171	1.1799	1.2628
13	0.4520	0.6883	0.7320	0.8435	1.0170	1.1799	1.2624
15	0.4517	0.6883	0.7320	0.8434	1.0170	1.1799	1.2621

TABLE V. Convergence study of frequency parameters, $\lambda' = \omega h \sqrt{\rho/E_2}$, for a five-ply square laminate with different degree of polynomial (p).

p	Mode shapes 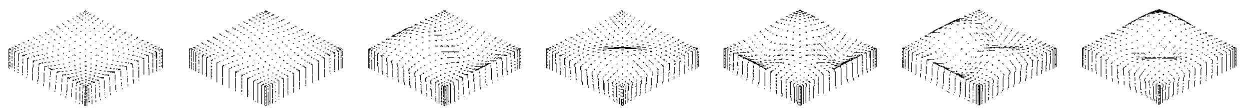						
7	0.4963	0.6883	0.8085	0.8778	1.1033	1.2468	1.2919
9	0.4955	0.6883	0.8082	0.8772	1.1021	1.2463	1.2907
11	0.4951	0.6883	0.8080	0.8769	1.1017	1.2462	1.2902
13	0.4949	0.6883	0.8080	0.8767	1.1015	1.2462	1.2899
15	0.4948	0.6883	0.8080	0.8765	1.1015	1.2462	1.2897

II. NUMERICAL STUDIES AND DISCUSSIONS

Several examples with various combinations of boundary conditions have been investigated to demonstrate the versatility of the p-Ritz method. All laminae have been assumed to have the same orthotropic properties and equal thicknesses. Numerical results from the published literature have been taken for comparison to demonstrate the accuracy of p-Ritz method integrated with the higher-order shear deformation theory. In this study, all results have been computed in double precision on a *SGI PowerChallenge* computer. Material properties used in all examples have been assumed to be nondimensional as follows:

Material 1: $E_1/E_2 = 1.0, \quad G_{12}/E_2 = (1+\nu)/2,$

$G_{23} = G_{13} = G_{12}, \quad \nu = 0.3.$

Material 2: $E_1/E_2 = 25, \quad G_{12}/E_2 = 0.5, \quad G_{23}/E_2 = 0.2,$

$G_{13} = G_{12}, \quad \nu_{12} = 0.25.$

Material 3: $E_1/E_2 = 40, \quad G_{12}/E_2 = 0.6, \quad G_{23}/E_2 = 0.5,$

$G_{13} = G_{12}, \quad \nu_{12} = 0.25.$

Material 4: $E_1/E_2 = 1.9\,040\,209,$

$G_{12}/E_2 = 0.5\,575\,868,$

$G_{23}/E_2 = 0.5\,658\,135,$

$G_{13} = 0.3\,391\,225, \quad \nu_{12} = 0.44.$

The present method has been verified using three examples with an aspect ratio $a/b = 1.0$ and boundary conditions of $S_3S_3S_3S_3$. The first example is an isotropic square plate of material 1 and with a length-to-thickness ratio $a/h = 10$, while the second and the third examples are three-ply and five-ply laminated plates of material 3 with $a/h = 5$ and stacking sequence (45°/−45°/45°) and (45°/−45°/45°/−45°/45°), respectively. A convergence study for frequency parameters was carried out by increasing the number of polynomials from 7 to 15. In Table III, the results for an isotropic plate[16] obtained using this method are very close to Noor's 3-D solutions[17] and Mallikarjuna's solutions[6] which were obtained by a higher-order theory and the finite element method. The frequency parameters obtained using $p = 9$ are within a discrepancy of 0.3% of $p = 15$ in all cases as shown in Tables III–V. It is observed that the fundamental frequencies for single-layer plates converge faster than those for the multi-layer laminates in Tables IV and V. The frequencies also converge rapidly for the modes dominated by in-plane displacements as opposed to the out-of-plane displacements. Higher values for p are therefore needed to provide sufficient accuracy for the higher modes. However, a higher p also leads to more computational effort. Therefore, the parameter $p = 15$ was adopted as a reasonable compromise for subsequent computation.

The fourth example presents a square plate made of ara-

TABLE VI. Comparison of frequency parameters, $\lambda' = \omega h \sqrt{\rho/E_1}$, for an orthotropic square plate made of Material 4.

Source	Mode shapes 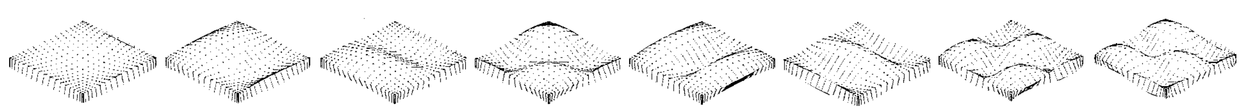							
CLPT	0.0493	0.1095	0.1327	0.1924	0.2070	0.2671	0.2879	0.3248
Mallikarjuna[6,a]	0.0473	0.1032	0.1190	0.1682	0.1906	0.2205	0.2432	0.2590
Mallikarjuna[6,b]	0.0474	0.1032	0.1190	0.1687	0.1903	0.2201	0.2450	0.2605
Present study	0.0474	0.1032	0.1188	0.1693	0.1885	0.2180	0.2471	0.2623
Reddy[5]	0.0474	0.1033	0.1189	0.1695	0.1888	0.2184	0.2477	0.2629
Srinivas[18]	0.0474	0.1033	0.1188	0.1694	0.1888	0.2180	0.2475	0.2624

[a]First-order shear deformation theory.
[b]Higher-order shear deformation theory.

TABLE VII. Effect of length-to-thickness ratio (a/h) on the fundamental frequency parameters, $\lambda' = (\omega a^2/h)\sqrt{\rho/E_2}$, for four-ply square plates of Material 3.

Source	a/h 4	5	10	20	50	100
CLPT	17.907	18.215	18.652	18.767	18.799	18.804
Rikards[7]	9.244	10.690	14.966	17.532	18.632	18.898
Mallikarjuna[6,a]	9.227	10.736	15.073	17.628	18.672	18.835
Mallikarjuna[6,b]	9.258	10.740	15.090	17.637	18.669	18.835
Present study	9.323	10.787	15.107	17.647	18.672	18.836
Reddy[5,b]	9.369	10.820	15.083	17.583	18.590	18.751
Reddy[5,c]	9.497	10.989	15.270	17.668	18.606	18.755

[a]First-order shear deformation theory.
[b]Higher-order shear deformation theory.
[c]Closed form solution.

gonite crystal with $a/h=10$ and boundary conditions of $S_3S_3S_3S_3$. The mode shapes and frequency parameters are tabulated in Table VI and compared with available results. While the results obtained by the present method have an error of less than 0.25% with respect to both Sriniva's 3-D solutions[18] and Reddy's closed form solutions,[5] the errors in the results from classical laminate plate theory (CLPT), Mallikarjuna[6] (first-order theory), and Mallikarjuna[6] (higher-order theory) are 23.78%, 1.73%, and 1.01% of the exact solutions. As expected, the results obtained by using present method are superior to those of CLPT and first-order theories. They are also very close to the closed form solutions and 3-D elasticity solutions. Therefore, the p-Ritz method is able to provide very accurate results without the difficulties of mesh generations and discretization losses in the finite element method.

In the fifth example, a four-ply square laminate made of material 3 stacked in a sequence of $(0°/90°)_s$ with boundary condition S_2 at all edges and a length-to-thickness ratio of 10 has been examined. The effect of the length-to-thickness ratio on the laminated plates has been presented in Table VII by varying the ratio from 4 to 100. As shown in Table VII, the effect of length-to-thickness ratio on the fundamental frequencies is pronounced and the error in using the classical laminated plate theory increases for thicker plates because of the neglect of shear effects. The present results are in close agreement with Reddy's closed form solutions.

The sixth example analyzed the same laminate as example 5 but with a length-to-thickness ratio of 5, different numbers of layers, and different degree of orthotropy. From the results in Table VIII, it is observed that the prediction of the fundamental frequency by CLPT is inaccurate for materials with a high degree of anisotropy. This reaffirms the fact that the effect of material anisotropy on the fundamental frequency for symmetrically laminated plates is pronounced. In addition, the response characteristics predicted by the present method are accurate and the maximum error in the fundamental frequencies is about 1% compared to the 3-D solutions of Noor.[17]

The effect of boundary conditions on the fundamental frequency has been examined in the seventh example. A four-ply square laminate made of material 3 has been as-

TABLE VIII. Effect of degree of orthotropy on the fundamental frequency, $\lambda' = \omega h\sqrt{\rho/E_2}$, for a square plates with $a/h=5$ and $S_2S_2S_2S_2$ edge conditions.

Source	Layers	E_1/E_2 3	10	20	30	40
CLPT	4	0.2920	0.4126	0.5404	0.6434	0.7320
Reddy[5]		0.2624	0.3309	0.3811	0.4109	0.4315
Present study		0.2624	0.3309	0.3811	0.4109	0.4315
Noor[17]		0.2647	0.3284	0.3824	0.4109	0.4301
CPT	5	0.2920	0.4126	0.5404	0.6434	0.7320
Mallikarjuna[6,a]		0.2626	0.3362	0.3919	0.4246	0.4463
Rikards[7]		0.2608	0.3313	0.3852	0.4142	0.4340
Mallikarjuna[6,b]		0.2626	0.3362	0.3919	0.4248	0.4470
Present study		0.2634	0.3372	0.3937	0.4274	0.4505
Noor[17]		0.2659	0.3409	0.3979	0.4314	0.4537
CPT	9	0.2920	0.4126	0.5404	0.6434	0.7320
Mallikarjuna[6,a]		0.2630	0.3404	0.4011	0.4376	0.4622
Mallikarjuna[6,b]		0.2630	0.3404	0.4011	0.4376	0.4622
Present study		0.2638	0.3413	0.4024	0.4395	0.4648
Noor[17]		0.2664	0.3443	0.4055	0.4421	0.4668

[a]First-order shear deformation theory.
[b]Higher-order shear deformation theory.

TABLE IX. Effect of boundary conditions on the fundamental frequency parameters, $\lambda' = (\omega a^2/h)\sqrt{\rho/E_2}$, for a four-ply square laminate of material 3.

Boundary conditions	Fundamental frequency parameter
$C_2F_2F_2F_2$	1.1378
$F_2F_2C_2F_2$	1.1378
$S_2F_4S_2F_4$	6.2185
$C_1F_4C_1F_4$	12.9422
$S_2S_2S_2S_2$	17.3813
$C_2S_2S_2S_2$	17.6704
$S_2S_2C_2S_2$	17.6704
$S_2C_2S_2C_2$	17.9726
$S_2C_1S_2C_1$	19.5025
$C_1C_1C_1C_1$	21.6722

sumed to have a length-to-thickness ratio of 10 and be stacked with a sequence of $(-45°/45°)_s$. As summarized in Table IX, the frequencies are higher for plates with stiffer constraints.

In the last two examples, the combined effects of plate aspect ratio, length-to-thickness ratio, and stacking angle for symmetric angle-ply, cantilevered $(C_1F_4F_4F_4,)$, and simply supported $(S_3S_3S_3S_3)$ laminated plate have been investigated. The laminates have been assumed to be made of material 3, and be either five-ply with stacking sequence $(\theta/-\theta/\theta/-\theta/\theta)$ or three-ply with stacking sequence $(\theta/-\theta/\theta)$. The

TABLE X. Effect of plate aspect ratio (a/b), length-to-thickness ratio (a/h), and lamination angle (θ) on the fundamental frequency parameters, $\lambda' = 100\times\omega h\sqrt{\rho/E_2}$, for laminated plates of material 3 with stacking sequence as $(\theta/-\theta/\theta/-\theta/\theta)$ and $C_1F_4F_4F_4$ edge conditions.

		a/b					
a/h	θ	0.2	0.5	1.0	2.0	5.0	10.0
5	15	15.9392	15.9138	15.7384	15.3293	14.6861	10.6903
	30	13.5254	13.3575	12.6835	11.5457	10.2224	5.8314
	45	10.1767	9.7417	8.5781	7.1679	6.1892	3.1327
	60	6.5221	6.0553	5.3839	4.8222	4.5297	2.2868
	75	4.2761	4.1890	4.1098	4.0619	4.0378	2.0629
	90	3.9612	3.9602	3.9596	3.9593	3.9591	2.0184
100	15	0.0574	0.0572	0.0567	0.0553	0.0525	0.0506
	30	0.0459	0.0451	0.0432	0.0396	0.0338	0.0302
	45	0.0315	0.0302	0.0277	0.0240	0.0192	0.0168
	60	0.0182	0.0172	0.0158	0.0142	0.0125	0.0118
	75	0.0111	0.0109	0.0107	0.0106	0.0104	0.0103
	90	0.0102	0.0102	0.0102	0.0102	0.0102	0.0102

TABLE XI. Effect of plate aspect ratio (a/b), length-to-thickness ratio (a/h), and lamination angle (θ) on the fundamental frequency parameters, $\lambda' = 100\times\omega h\sqrt{\rho/E_2}$, for laminated plates with stacking sequence as $(\theta/-\theta/\theta)$ and $S_3S_3S_3S_3$ edge conditions.

		a/b							
		Material 2				Material 3			
a/h	θ	0.5	1.0	1.5	2.0	0.5	1.0	1.5	2.0
5	15°	32.2071	35.8155	42.6236	52.0862	37.6402	41.6871	49.7996	61.5597
	30°	29.2007	36.2748	46.6866	58.8802	35.3459	44.0053	56.8605	72.1304
	45°	25.6464	36.6625	50.3993	66.1334	31.6364	45.1748	62.2065	81.8287
	60°	22.1526	36.2748	53.6901	72.9672	26.8135	44.0053	64.5530	87.0976
	75°	18.5448	35.8155	56.3615	78.2015	21.5853	41.6871	64.8946	89.6031
10	15°	11.2081	12.4525	14.9253	18.5448	13.5798	14.8732	17.5509	21.5853
	30°	9.8742	12.6714	16.9729	22.1526	12.1558	15.4325	20.5688	26.8135
	45°	8.3602	12.8639	18.7282	25.6464	10.2682	15.7841	23.0298	31.6364
	60°	6.9411	12.6714	20.3417	29.2007	8.3294	15.4325	24.7607	35.3459
	75°	5.5211	12.4525	21.8693	32.2071	6.4265	14.8732	25.8619	37.6402
20	15°	3.2341	3.6033	4.3657	5.5211	4.0139	4.3921	5.1914	6.4265
	30°	2.8157	3.7035	5.1364	6.9411	3.4941	4.5186	6.2016	8.3294
	45°	2.3346	3.7827	5.8106	8.3602	2.8587	4.6234	7.1143	10.2682
	60°	1.8917	3.7035	6.4131	9.8742	2.2622	4.5186	7.8871	12.1558
	75°	1.4674	3.6033	6.9919	11.2081	1.7097	4.3921	8.5389	13.5798
30	15°	1.4851	1.6566	2.0151	2.5644	1.8549	2.0306	2.4044	2.9870
	30°	1.2901	1.7094	2.3977	3.2813	1.6036	2.0862	2.8919	3.9277
	45°	1.0642	1.7502	2.7378	4.0187	1.3021	2.1367	3.3465	4.9257
	60°	0.8569	1.7094	3.0360	4.8157	1.0240	2.0862	3.7443	5.9624
	75°	0.6607	1.6566	3.3187	5.5135	0.7700	2.0306	4.0998	6.7906
40	15°	0.8455	0.9437	1.1499	1.4674	1.0586	1.1592	1.3739	1.7097
	30°	0.7334	0.9755	1.3748	1.8917	0.9129	1.1907	1.6575	2.2622
	45°	0.6043	0.9999	1.5762	2.3346	0.7392	1.2201	1.9252	2.8587
	60°	0.4854	0.9755	1.7509	2.8157	0.5800	1.1907	2.1616	3.4941
	75°	0.3734	0.9437	1.9152	3.2341	0.4353	1.1592	2.3776	4.0139
50	15°	0.5442	0.6076	0.7411	0.9470	0.6822	0.7472	0.8860	1.1035
	30°	0.4723	0.6287	0.8881	1.2255	0.5876	0.7674	1.0706	1.4649
	45°	0.3886	0.6448	1.0203	1.5185	0.4752	0.7867	1.2459	1.8584
	60°	0.3117	0.6287	1.1343	1.8374	0.3724	0.7674	1.4011	2.2826
	75°	0.2395	0.6076	1.2411	2.1135	0.2792	0.7472	1.5444	2.6337

results are presented in Tables X and XI. In both examples, the fundamental frequencies decrease with an increase in length-to-thickness ratio. It is observed that boundary conditions have a significant influence on the effect of stacking angle for laminated plates. As shown in Table XI, for the simply supported laminates, the fundamental frequencies decrease as stacking angle increases for a plate with $a/b < 1.0$, and increase for $a/b > 1.0$. However, for cantilevered laminates, the fundamental frequencies decrease as the stacking angle increases. It has also been shown that the fundamental frequencies increase with aspect ratio for simply supported laminates and decrease with aspect ratio for cantilevered laminates.

III. CONCLUSIONS

The p-Ritz method has been employed for free vibration analysis of thick composite plates with symmetric lamination based on the higher-order shear deformation theory. A concise governing eigenvalue equation has been derived. Convergence of eigenvalues has been verified and excellent agreement has been achieved with respect to first-order, higher-order, finite element, and three-dimensional elasticity solutions. Numerical frequencies for laminates made of materials with different degrees of orthotropy have been presented and illustrated with relevant vibration mode shapes. The effect of length-to-thickness ratio, boundary conditions, plate aspect ratio, number of layers, and stacking angles on the laminates have also been investigated. This analysis suggests that, so far as the free vibration of laminated composite plate is concerned, the higher-order shear deformation theory is able to predict accurate solutions. The versatility of the p-Ritz method in accounting for laminated plates with a variety of boundary constraints should be appreciated.

APPENDIX

Substitution of Eqs. (1a)–(1c), (2), (4), and (10) into Eqs. (8) and (9) yields

$$
\begin{aligned}
U=\frac{1}{2}\int\int_A\Bigg\{ & A_{55}\phi_x^2+D_{11}\left(\frac{\partial\phi_x}{\partial x}\right)^2+2D_{16}\left(\frac{\partial\phi_x}{\partial x}\right)\left(\frac{\partial\phi_x}{\partial y}\right)+D_{66}\left(\frac{\partial\phi_x}{\partial y}\right)^2+2A_{45}\phi_x\phi_y+A_{44}\phi_y^2+2D_{16}\left(\frac{\partial\phi_x}{\partial x}\right)\left(\frac{\partial\phi_y}{\partial x}\right)\\
&+2D_{66}\left(\frac{\partial\phi_x}{\partial y}\right)\left(\frac{\partial\phi_y}{\partial x}\right)+D_{66}\left(\frac{\partial\phi_y}{\partial x}\right)^2+2D_{12}\left(\frac{\partial\phi_x}{\partial x}\right)\left(\frac{\partial\phi_y}{\partial y}\right)+2D_{26}\left(\frac{\partial\phi_x}{\partial y}\right)\left(\frac{\partial\phi_y}{\partial y}\right)+2D_{26}\left(\frac{\partial\phi_y}{\partial x}\right)\left(\frac{\partial\phi_y}{\partial y}\right)+D_{22}\left(\frac{\partial\phi_y}{\partial y}\right)^2\\
&+F_{44}\left(\frac{16}{h^4}\right)\phi_y^2+F_{45}\left(\frac{32}{h^4}\right)\phi_x\phi_y+F_{55}\left(\frac{16}{h^4}\right)\phi_x^2-D_{55}\left(\frac{8}{h^2}\right)\phi_x^2-D_{45}\left(\frac{16}{h^2}\right)\phi_x\phi_y-F_{16}\left(\frac{16}{3h^2}\right)\left(\frac{\partial\phi_x}{\partial x}\right)\left(\frac{\partial\phi_y}{\partial x}\right)-F_{12}\left(\frac{16}{3h^2}\right)\\
&\times\left(\frac{\partial\phi_x}{\partial x}\right)\left(\frac{\partial\phi_y}{\partial y}\right)-F_{16}\left(\frac{16}{3h^2}\right)\left(\frac{\partial\phi_x}{\partial x}\right)\left(\frac{\partial\phi_x}{\partial y}\right)-D_{44}\left(\frac{8}{h^2}\right)\phi_y^2-F_{11}\left(\frac{8}{3h^2}\right)\left(\frac{\partial\phi_x}{\partial x}\right)^2-F_{22}\left(\frac{8}{3h^2}\right)\left(\frac{\partial\phi_y}{\partial y}\right)^2-F_{26}\left(\frac{16}{3h^2}\right)\left(\frac{\partial\phi_x}{\partial y}\right)\\
&\times\left(\frac{\partial\phi_y}{\partial y}\right)-F_{26}\left(\frac{16}{3h^2}\right)\left(\frac{\partial\phi_y}{\partial x}\right)\left(\frac{\partial\phi_y}{\partial y}\right)-F_{66}\left(\frac{8}{3h^2}\right)\left(\frac{\partial\phi_x}{\partial y}\right)^2+A_{11}\left(\frac{\partial u_0}{\partial x}\right)^2-F_{66}\left(\frac{16}{3h^2}\right)\left(\frac{\partial\phi_x}{\partial y}\right)\left(\frac{\partial\phi_y}{\partial x}\right)-F_{66}\left(\frac{8}{3h^2}\right)\left(\frac{\partial\phi_y}{\partial x}\right)^2\\
&+H_{11}\left(\frac{16}{9h^4}\right)\left(\frac{\partial\phi_x}{\partial x}\right)^2+H_{12}\left(\frac{32}{9h^4}\right)\left(\frac{\partial\phi_x}{\partial x}\right)\left(\frac{\partial\phi_y}{\partial y}\right)+H_{16}\left(\frac{32}{9h^4}\right)\left(\frac{\partial\phi_x}{\partial x}\right)\left(\frac{\partial\phi_x}{\partial y}\right)+2A_{16}\left(\frac{\partial u_0}{\partial x}\right)\left(\frac{\partial v_0}{\partial x}\right)+H_{16}\left(\frac{32}{9h^4}\right)\left(\frac{\partial\phi_x}{\partial x}\right)\\
&\times\left(\frac{\partial\phi_y}{\partial x}\right)+H_{22}\left(\frac{16}{9h^4}\right)\left(\frac{\partial\phi_y}{\partial y}\right)^2+H_{26}\left(\frac{32}{9h^4}\right)\left(\frac{\partial\phi_x}{\partial y}\right)\left(\frac{\partial\phi_y}{\partial y}\right)+H_{26}\left(\frac{32}{9h^4}\right)\left(\frac{\partial\phi_y}{\partial y}\right)\left(\frac{\partial\phi_y}{\partial x}\right)+H_{66}\left(\frac{16}{9h^4}\right)\left(\frac{\partial\phi_x}{\partial y}\right)^2\\
&+H_{66}\left(\frac{32}{9h^4}\right)\left(\frac{\partial\phi_x}{\partial y}\right)\left(\frac{\partial\phi_y}{\partial x}\right)+H_{66}\left(\frac{16}{9h^4}\right)\left(\frac{\partial\phi_y}{\partial x}\right)^2+A_{66}\left(\frac{\partial v_0}{\partial x}\right)^2+2A_{16}\left(\frac{\partial u_0}{\partial x}\right)\left(\frac{\partial u_0}{\partial y}\right)+A_{66}\left(\frac{\partial u_0}{\partial y}\right)^2+2A_{66}\left(\frac{\partial u_0}{\partial y}\right)\left(\frac{\partial v_0}{\partial x}\right)\\
&+2A_{12}\left(\frac{\partial u_0}{\partial x}\right)\left(\frac{\partial v_0}{\partial y}\right)+A_{22}\left(\frac{\partial v_0}{\partial y}\right)^2+2A_{26}\left(\frac{\partial u_0}{\partial y}\right)\left(\frac{\partial v_0}{\partial y}\right)+2A_{26}\left(\frac{\partial v_0}{\partial x}\right)\left(\frac{\partial v_0}{\partial y}\right)+2A_{55}\phi_x\left(\frac{\partial w_0}{\partial x}\right)+2A_{45}\phi_y\left(\frac{\partial w_0}{\partial x}\right)\\
&+F_{45}\left(\frac{32}{h^4}\right)\phi_y\left(\frac{\partial w_0}{\partial x}\right)+F_{55}\left(\frac{32}{h^4}\right)\phi_x\left(\frac{\partial w_0}{\partial x}\right)-D_{55}\left(\frac{16}{h^2}\right)\phi_x\left(\frac{\partial w_0}{\partial x}\right)-D_{45}\left(\frac{16}{h^2}\right)\phi_y\left(\frac{\partial w_0}{\partial x}\right)+A_{55}\left(\frac{\partial w_0}{\partial x}\right)^2+F_{55}\left(\frac{16}{h^4}\right)\left(\frac{\partial w_0}{\partial x}\right)^2\\
&-F_{11}\left(\frac{8}{3h^2}\right)\left(\frac{\partial\phi_x}{\partial x}\right)\left(\frac{\partial^2 w_0}{\partial x^2}\right)+H_{16}\left(\frac{32}{9h^4}\right)\left(\frac{\partial\phi_y}{\partial x}\right)\left(\frac{\partial^2 w_0}{\partial x^2}\right)-F_{12}\left(\frac{8}{3h^2}\right)\left(\frac{\partial\phi_y}{\partial y}\right)\left(\frac{\partial^2 w_0}{\partial x^2}\right)-F_{16}\left(\frac{8}{3h^2}\right)\left(\frac{\partial\phi_x}{\partial y}\right)\left(\frac{\partial^2 w_0}{\partial x^2}\right)\\
&+2A_{45}\phi_x\left(\frac{\partial w_0}{\partial y}\right)-F_{16}\left(\frac{8}{3h^2}\right)\left(\frac{\partial\phi_y}{\partial x}\right)\left(\frac{\partial^2 w_0}{\partial x^2}\right)+H_{11}\left(\frac{32}{9h^4}\right)\left(\frac{\partial\phi_x}{\partial x}\right)\left(\frac{\partial^2 w_0}{\partial x^2}\right)+2A_{44}\phi_y\left(\frac{\partial w_0}{\partial y}\right)+H_{12}\left(\frac{32}{9h^4}\right)\left(\frac{\partial\phi_y}{\partial y}\right)\left(\frac{\partial^2 w_0}{\partial x^2}\right)\\
&+H_{16}\left(\frac{32}{9h^4}\right)\left(\frac{\partial\phi_x}{\partial y}\right)\left(\frac{\partial^2 w_0}{\partial x^2}\right)+H_{11}\left(\frac{16}{9h^4}\right)\left(\frac{\partial^2 w_0}{\partial x^2}\right)^2-D_{44}\left(\frac{8}{h^4}\right)\left(\frac{\partial w_0}{\partial y}\right)^2-F_{16}\left(\frac{16}{3h^2}\right)\left(\frac{\partial\phi_x}{\partial x}\right)\left(\frac{\partial^2 w_0}{\partial x\,\partial y}\right)
\end{aligned}
$$

$$-F_{26}\left(\frac{16}{3h^2}\right)\left(\frac{\partial \phi_y}{\partial y}\right)\left(\frac{\partial^2 w_0}{\partial x\ \partial y}\right)-F_{66}\left(\frac{16}{3h^2}\right)\left(\frac{\partial \phi_x}{\partial y}\right)\left(\frac{\partial^2 w_0}{\partial x\ \partial y}\right)-F_{66}\left(\frac{16}{3h^2}\right)\left(\frac{\partial \phi_y}{\partial x}\right)\left(\frac{\partial^2 w_0}{\partial x\ \partial y}\right)-D_{55}\left(\frac{8}{h^2}\right)\left(\frac{\partial w_0}{\partial x}\right)^2$$

$$+H_{16}\left(\frac{64}{9h^4}\right)\left(\frac{\partial \phi_x}{\partial x}\right)\left(\frac{\partial^2 w_0}{\partial x\ \partial y}\right)+H_{26}\left(\frac{64}{9h^4}\right)\left(\frac{\partial \phi_y}{\partial y}\right)\left(\frac{\partial^2 w_0}{\partial x\ \partial y}\right)+A_{44}\left(\frac{\partial w_0}{\partial y}\right)^2+H_{66}\left(\frac{64}{9h^4}\right)\left(\frac{\partial \phi_x}{\partial y}\right)\left(\frac{\partial^2 w_0}{\partial x\ \partial y}\right)$$

$$+H_{66}\left(\frac{64}{9h^4}\right)\left(\frac{\partial \phi_y}{\partial x}\right)\left(\frac{\partial^2 w_0}{\partial x\ \partial y}\right)+F_{44}\left(\frac{16}{h^4}\right)\left(\frac{\partial w_0}{\partial y}\right)^2-H_{16}\left(\frac{64}{9h^4}\right)\left(\frac{\partial^2 w_0}{\partial x^2}\right)\left(\frac{\partial^2 w_0}{\partial x\ \partial y}\right)+H_{66}\left(\frac{64}{9h^4}\right)\left(\frac{\partial^2 w_0}{\partial x\ \partial y}\right)^2$$

$$+F_{44}\left(\frac{32}{h^4}\right)\phi_y\left(\frac{\partial w_0}{\partial y}\right)+2A_{45}\left(\frac{\partial w_0}{\partial x}\right)\left(\frac{\partial w_0}{\partial y}\right)+F_{45}\left(\frac{32}{h^4}\right)\left(\frac{\partial w_0}{\partial x}\right)\left(\frac{\partial w_0}{\partial y}\right)-D_{45}\left(\frac{16}{h^2}\right)\left(\frac{\partial w_0}{\partial x}\right)\left(\frac{\partial w_0}{\partial y}\right)-F_{12}\left(\frac{8}{3h^2}\right)\left(\frac{\partial \phi_x}{\partial x}\right)$$

$$\times\left(\frac{\partial^2 w_0}{\partial y^2}\right)-F_{22}\left(\frac{8}{3h^2}\right)\left(\frac{\partial \phi_y}{\partial y}\right)\left(\frac{\partial^2 w_0}{\partial y^2}\right)-D_{45}\left(\frac{16}{h^2}\right)\phi_x\left(\frac{\partial w_0}{\partial y}\right)-F_{26}\left(\frac{8}{3h^2}\right)\left(\frac{\partial \phi_x}{\partial y}\right)\left(\frac{\partial^2 w_0}{\partial y^2}\right)-F_{26}\left(\frac{8}{3h^2}\right)\left(\frac{\partial \phi_y}{\partial x}\right)\left(\frac{\partial^2 w_0}{\partial y^2}\right)$$

$$+F_{45}\left(\frac{32}{h^4}\right)\phi_x\left(\frac{\partial w_0}{\partial y}\right)-H_{12}\left(\frac{32}{9h^4}\right)\left(\frac{\partial \phi_x}{\partial x}\right)\left(\frac{\partial^2 w_0}{\partial y^2}\right)+H_{22}\left(\frac{32}{9h^4}\right)\left(\frac{\partial \phi_y}{\partial y}\right)\left(\frac{\partial^2 w_0}{\partial y^2}\right)-D_{44}\left(\frac{16}{h^2}\right)\phi_y\left(\frac{\partial w_0}{\partial y}\right)+H_{26}\left(\frac{32}{9h^4}\right)\left(\frac{\partial \phi_x}{\partial y}\right)$$

$$\times\left(\frac{\partial^2 w_0}{\partial y^2}\right)+H_{26}\left(\frac{32}{9h^4}\right)\left(\frac{\partial \phi_y}{\partial x}\right)\left(\frac{\partial^2 w_0}{\partial y^2}\right)+H_{22}\left(\frac{16}{9h^4}\right)\left(\frac{\partial^2 w_0}{\partial y^2}\right)^2-H_{12}\left(\frac{32}{9h^4}\right)\left(\frac{\partial^2 w_0}{\partial x^2}\right)\left(\frac{\partial^2 w_0}{\partial y^2}\right)$$

$$+H_{26}\left(\frac{64}{9h^4}\right)\left(\frac{\partial^2 w_0}{\partial x\ \partial y}\right)\left(\frac{\partial^2 w_0}{\partial y^2}\right)\Bigg\}\ dA. \tag{A1}$$

If the laminae are made of the same material with mass density per unit volume ρ, the total kinetic energy becomes

$$T=\frac{\rho\omega^2}{2}\int\int_A\left\{\frac{h^3}{315}\left(17\phi_x^2+17\phi_y^2-8\,\phi_x\,\frac{\partial w_0}{\partial x}-8\,\phi_y\,\frac{\partial w_0}{\partial y}\right)+h(u_0^2+v_0^2+w_0^2)+\frac{h^3}{252}\,(\phi_x^2+\phi_y^2)\right\}\ dA. \tag{A2}$$

The stiffness matrices $\mathbf{K}$ and the mass matrices $\mathbf{M}$ are given by

$$\mathbf{K}=\frac{1}{D_0}\begin{bmatrix}[\mathbf{K}^{uu}] & [\mathbf{K}^{uv}] & 0 & 0 & 0\\ & [\mathbf{K}^{vv}] & 0 & 0 & 0\\ & & [\mathbf{K}^{ww}] & [\mathbf{K}^{w\theta_u}] & [\mathbf{K}^{w\theta_v}]\\ & \text{sym.} & & [\mathbf{K}^{\theta_u\theta_u}] & [\mathbf{K}^{\theta_u\theta_v}]\\ & & & & [\mathbf{K}^{\theta_v\theta_v}]\end{bmatrix} \tag{A3}$$

and

$$\mathbf{M}=\begin{bmatrix}[\mathbf{M}^{uu}] & 0 & 0 & 0 & 0\\ & [\mathbf{M}^{vv}] & 0 & 0 & 0\\ & & [\mathbf{M}^{ww}] & [\mathbf{M}^{w\theta_u}] & [\mathbf{M}^{w\theta_v}]\\ & \text{sym.} & & [\mathbf{M}^{\theta_u\theta_u}] & 0\\ & & & & [\mathbf{M}^{\theta_v\theta_v}]\end{bmatrix}, \tag{A4}$$

where the elements of $\mathbf{K}$ and $\mathbf{M}$ can further be expressed as

$$\mathbf{K}_{ij}^{uu}=A_{66}\left(\frac{a^2}{h^3}\right)\mathbf{R}_{\varphi_i^u\varphi_j^u}^{0101}+A_{16}\left(\frac{ab}{h^3}\right)[\mathbf{R}_{\varphi_i^u\varphi_j^u}^{0110}+\mathbf{R}_{\varphi_i^u\varphi_j^u}^{1001}]+A_{11}\left(\frac{b^2}{h^3}\right)\mathbf{R}_{\varphi_i^u\varphi_j^u}^{1010}, \tag{A5a}$$

$$\mathbf{K}_{ij}^{uv}=A_{26}\left(\frac{a^2}{h^3}\right)\mathbf{R}_{\varphi_i^u\varphi_j^v}^{0101}+\left(\frac{ab}{h^3}\right)[A_{66}\mathbf{R}_{\varphi_i^u\varphi_j^v}^{0110}+A_{12}\mathbf{R}_{\varphi_i^u\varphi_j^v}^{1001}]+A_{16}\left(\frac{b^2}{h^3}\right)\mathbf{R}_{\varphi_i^u\varphi_j^v}^{1010}, \tag{A5b}$$

$$\mathbf{K}_{ij}^{vv}=A_{22}\left(\frac{a^2}{h^3}\right)\mathbf{R}_{\varphi_i^v\varphi_j^v}^{0101}+A_{26}\left(\frac{ab}{h^3}\right)[\mathbf{R}_{\varphi_i^v\varphi_j^v}^{0110}+\mathbf{R}_{\varphi_i^v\varphi_j^v}^{1001}]+A_{66}\left(\frac{b^2}{h^3}\right)\mathbf{R}_{\varphi_i^v\varphi_j^v}^{1010}, \tag{A5c}$$

$$
\begin{aligned}
\mathbf{K}_{ij}^{ww}=&\left[A_{44}\left(\frac{a^2}{h^3}\right)-D_{44}\left(\frac{8a^2}{h^5}\right)+F_{44}\left(\frac{16a^2}{h^7}\right)\right]\mathbf{R}_{\varphi_i^w\varphi_j^w}^{0101}+\left[A_{45}\left(\frac{ab}{h^3}\right)-D_{45}\left(\frac{8ab}{h^5}\right)+F_{45}\left(\frac{16ab}{h^7}\right)\right][\mathbf{R}_{\varphi_i^w\varphi_j^w}^{0110}+\mathbf{R}_{\varphi_i^w\varphi_j^w}^{1001}]+\left[A_{55}\left(\frac{b^2}{h^3}\right)\right.\\
&\left.-D_{55}\left(\frac{8b^2}{h^5}\right)+F_{55}\left(\frac{16b^2}{h^7}\right)\right]\mathbf{R}_{\varphi_i^w\varphi_j^w}^{1010}+H_{22}\left(\frac{16a^2}{9b^2h^7}\right)\mathbf{R}_{\varphi_i^w\varphi_j^w}^{0202}+H_{26}\left(\frac{32a}{9bh^7}\right)[\mathbf{R}_{\varphi_i^w\varphi_j^w}^{0211}+\mathbf{R}_{\varphi_i^w\varphi_j^w}^{1102}]+H_{66}\left(\frac{64}{9h^7}\right)\mathbf{R}_{\varphi_i^w\varphi_j^w}^{1111}\\
&+H_{16}\left(\frac{32b}{9ah^7}\right)[\mathbf{R}_{\varphi_i^w\varphi_j^w}^{1120}+\mathbf{R}_{\varphi_i^w\varphi_j^w}^{2011}]+H_{12}\left(\frac{16}{9h^7}\right)[\mathbf{R}_{\varphi_i^w\varphi_j^w}^{0220}+\mathbf{R}_{\varphi_i^w\varphi_j^w}^{2002}]+H_{11}\left(\frac{16b^2}{9a^2h^7}\right)\mathbf{R}_{\varphi_i^w\varphi_j^w}^{2020},
\end{aligned}
\tag{A5d}
$$

$$
\begin{aligned}
\mathbf{K}_{ij}^{w\theta_u}=&\left[A_{45}\left(\frac{ab}{h^3}\right)-D_{45}\left(\frac{8ab}{h^5}\right)+F_{45}\left(\frac{16ab}{h^7}\right)\right]\mathbf{R}_{\varphi_i^w\varphi_j^{\theta_u}}^{0100}+\left[H_{26}\left(\frac{16a}{9bh^7}\right)-F_{26}\left(\frac{4a}{3bh^5}\right)\right]\mathbf{R}_{\varphi_i^w\varphi_j^{\theta_u}}^{0201}+\left[H_{12}\left(\frac{16}{9h^7}\right)\right.\\
&\left.-F_{12}\left(\frac{4}{3h^5}\right)\right]\mathbf{R}_{\varphi_i^w\varphi_j^{\theta_u}}^{0210}+\left[A_{55}\left(\frac{b^2}{h^3}\right)-D_{55}\left(\frac{8b^2}{h^5}\right)+F_{55}\left(\frac{16b^2}{h^7}\right)\right]\mathbf{R}_{\varphi_i^w\varphi_j^{\theta_u}}^{1000}+\left[H_{66}\left(\frac{32}{9h^7}\right)-F_{66}\left(\frac{8}{3h^5}\right)\right]\mathbf{R}_{\varphi_i^w\varphi_j^{\theta_u}}^{1101}\\
&+\left[H_{16}\left(\frac{16b}{9ah^7}\right)-F_{16}\left(\frac{4b}{3ah^5}\right)\right][2\mathbf{R}_{\varphi_i^w\varphi_j^{\theta_u}}^{1110}+\mathbf{R}_{\varphi_i^w\varphi_j^{\theta_u}}^{2001}]+\left[H_{11}\left(\frac{16b^2}{9a^2h^7}\right)-F_{11}\left(\frac{4b^2}{3a^2h^5}\right)\right]\mathbf{R}_{\varphi_i^w\varphi_j^{\theta_u}}^{2010},
\end{aligned}
\tag{A5e}
$$

$$
\begin{aligned}
\mathbf{K}_{ij}^{w\theta_v}=&\left[A_{44}\left(\frac{a^2}{h^3}\right)-D_{44}\left(\frac{8a^2}{h^5}\right)+F_{44}\left(\frac{16a^2}{h^7}\right)\right]\mathbf{R}_{\varphi_i^w\varphi_j^{\theta_v}}^{0100}+\left[H_{22}\left(\frac{16a^2}{9b^2h^7}\right)-F_{22}\left(\frac{4a^2}{3b^2h^5}\right)\right]\mathbf{R}_{\varphi_i^w\varphi_j^{\theta_v}}^{0201}+\left[H_{26}\left(\frac{16a}{9bh^7}\right)\right.\\
&\left.-F_{26}\left(\frac{4a}{3bh^5}\right)\right]\mathbf{R}_{\varphi_i^w\varphi_j^{\theta_v}}^{0210}+\left[A_{45}\left(\frac{ab}{h^3}\right)-D_{45}\left(\frac{8ab}{h^5}\right)+F_{45}\left(\frac{16ab}{h^7}\right)\right]\mathbf{R}_{\varphi_i^w\varphi_j^{\theta_v}}^{1000}+\left[H_{26}\left(\frac{32a}{9bh^7}\right)-F_{26}\left(\frac{8a}{3bh^5}\right)\right]\mathbf{R}_{\varphi_i^w\varphi_j^{\theta_v}}^{1101}\\
&+\left[H_{66}\left(\frac{32}{9h^7}\right)-F_{66}\left(\frac{8}{3h^5}\right)\right]\mathbf{R}_{\varphi_i^w\varphi_j^{\theta_v}}^{1110}+\left[H_{12}\left(\frac{16}{9h^7}\right)-F_{12}\left(\frac{4}{3h^5}\right)\right]\mathbf{R}_{\varphi_i^w\varphi_j^{\theta_v}}^{2001}+\left[H_{16}\left(\frac{16b}{9ah^7}\right)-F_{16}\left(\frac{4b}{3ah^5}\right)\right]\mathbf{R}_{\varphi_i^w\varphi_j^{\theta_v}}^{2010},
\end{aligned}
\tag{A5f}
$$

$$
\begin{aligned}
\mathbf{K}_{ij}^{\theta_u\theta_u}=&\left[A_{55}\left(\frac{b^2}{h^3}\right)-D_{55}\left(\frac{8b^2}{h^5}\right)+F_{55}\left(\frac{16b^2}{h^7}\right)\right]\mathbf{R}_{\varphi_i^{\theta_u}\varphi_j^{\theta_u}}^{0000}+\left[D_{66}\left(\frac{1}{h^3}\right)+H_{66}\left(\frac{16}{9h^7}\right)-F_{66}\left(\frac{8}{3h^5}\right)\right]\mathbf{R}_{\varphi_i^{\theta_u}\varphi_j^{\theta_u}}^{0101}+\left[D_{16}\left(\frac{b}{ah^3}\right)\right.\\
&\left.+H_{16}\left(\frac{16b}{9ah^7}\right)-F_{16}\left(\frac{8b}{3ah^5}\right)\right][\mathbf{R}_{\varphi_i^{\theta_u}\varphi_j^{\theta_u}}^{0110}+\mathbf{R}_{\varphi_i^{\theta_u}\varphi_j^{\theta_u}}^{1001}]+\left[D_{11}\left(\frac{b^2}{a^2h^3}\right)+H_{11}\left(\frac{16b^2}{9a^2h^7}\right)-F_{11}\left(\frac{8b^2}{3a^2h^5}\right)\right]\mathbf{R}_{\varphi_i^{\theta_u}\varphi_j^{\theta_u}}^{1010},
\end{aligned}
\tag{A5g}
$$

$$
\begin{aligned}
\mathbf{K}_{ij}^{\theta_u\theta_v}=&\left[A_{45}\left(\frac{ab}{h^3}\right)-D_{45}\left(\frac{8ab}{h^5}\right)+F_{45}\left(\frac{16ab}{h^7}\right)\right]\mathbf{R}_{\varphi_i^{\theta_u}\varphi_j^{\theta_v}}^{0000}+\left[D_{26}\left(\frac{a}{bh^3}\right)+H_{26}\left(\frac{16a}{9bh^7}\right)-F_{26}\left(\frac{8a}{3bh^5}\right)\right]\mathbf{R}_{\varphi_i^{\theta_u}\varphi_j^{\theta_v}}^{0101}\\
&+\left[D_{66}\left(\frac{1}{h^3}\right)+H_{66}\left(\frac{16}{9h^7}\right)-F_{66}\left(\frac{8}{3h^5}\right)\right]\mathbf{R}_{\varphi_i^{\theta_u}\varphi_j^{\theta_v}}^{0110}+\left[D_{12}\left(\frac{1}{h^3}\right)+H_{12}\left(\frac{16}{9h^7}\right)-F_{12}\left(\frac{8}{3h^5}\right)\right]\mathbf{R}_{\varphi_i^{\theta_u}\varphi_j^{\theta_v}}^{1001}\\
&+\left[D_{16}\left(\frac{b}{ah^3}\right)+H_{16}\left(\frac{16b}{9ah^7}\right)-F_{16}\left(\frac{8b}{3ah^5}\right)\right]\mathbf{R}_{\varphi_i^{\theta_u}\varphi_j^{\theta_v}}^{1010},
\end{aligned}
\tag{A5h}
$$

$$
\begin{aligned}
\mathbf{K}_{ij}^{\theta_v\theta_v}=&\left[A_{44}\left(\frac{a^2}{h^3}\right)-D_{44}\left(\frac{8a^2}{h^5}\right)+F_{44}\left(\frac{16a^2}{h^7}\right)\right]\mathbf{R}_{\varphi_i^{\theta_v}\varphi_j^{\theta_v}}^{0000}+\left[D_{22}\left(\frac{a^2}{b^2h^3}\right)+H_{22}\left(\frac{16a^2}{9b^2h^7}\right)-F_{22}\left(\frac{8a^2}{3b^2h^5}\right)\right]\mathbf{R}_{\varphi_i^{\theta_v}\varphi_j^{\theta_v}}^{0101}+\left[D_{26}\left(\frac{a}{bh^3}\right)\right.\\
&\left.+H_{26}\left(\frac{16a}{9bh^7}\right)-F_{26}\left(\frac{8a}{3bh^5}\right)\right][\mathbf{R}_{\varphi_i^{\theta_v}\varphi_j^{\theta_v}}^{0110}+\mathbf{R}_{\varphi_i^{\theta_v}\varphi_j^{\theta_v}}^{1001}]+\left[D_{66}\left(\frac{1}{h^3}\right)+H_{66}\left(\frac{16}{9h^7}\right)-F_{66}\left(\frac{8}{3h^5}\right)\right]\mathbf{R}_{\varphi_i^{\theta_v}\varphi_j^{\theta_v}}^{1010},
\end{aligned}
\tag{A5i}
$$

and

$$\mathbf{M}_{ij}^{uu}=h\mathbf{R}_{\varphi_i^u\varphi_j^u}^{0000}, \tag{A6a}$$

$$\mathbf{M}_{ij}^{vv}=h\mathbf{R}_{\varphi_i^v\varphi_j^v}^{0000}, \tag{A6b}$$

$$\mathbf{M}_{ij}^{ww}=h\mathbf{R}_{\varphi_i^w\varphi_j^w}^{0000}+\left(\frac{h^3}{252b^2}\right)\mathbf{R}_{\varphi_i^w\varphi_j^w}^{0101}+\left(\frac{h^3}{252a^2}\right)\mathbf{R}_{\varphi_i^w\varphi_j^w}^{1010}, \tag{A6c}$$

$$\mathbf{M}_{ij}^{w\theta_u}=\left(\frac{-4h^3}{315a^2}\right)\mathbf{R}_{\varphi_i^w\varphi_j^{\theta_u}}^{1000}, \tag{A6d}$$

$$\mathbf{M}_{ij}^{w\theta_v}=\left(\frac{-4h^3}{315b^2}\right)\mathbf{R}_{\varphi_i^w\varphi_j^{\theta_v}}^{0100}, \tag{A6e}$$

$$\mathbf{M}_{ij}^{\theta_u\theta_u}=\left(\frac{17h^3}{315a^2}\right)\mathbf{R}_{\varphi_i^{\theta_u}\varphi_j^{\theta_u}}^{0000}, \tag{A6f}$$

$$\mathbf{M}_{ij}^{\theta_v\theta_v}=\left(\frac{17h^3}{315b^2}\right)\mathbf{R}_{\varphi_i^{\theta_v}\varphi_j^{\theta_v}}^{0000}, \tag{A6g}$$

in which

$$\mathbf{R}^{defg}_{\varphi_i^\alpha \theta_j^\beta} = \int \int_A \frac{\partial^{d+e} \varphi_i^\alpha(\xi,\eta)}{\partial \xi^d \, \partial \eta^e} \frac{\partial^{f+g} \theta_j^\beta(\xi,\eta)}{\partial \xi^f \, \partial \eta^g} \, d\xi \, d\eta. \tag{A7}$$

[1] P. C. Yang, C. H. Norris, and Y. Stavsky, ''Elastic wave propagation in heterogeneous plates,'' Int. J. Solids Struct. **2**, 665–684 (1966).

[2] J. N. Reddy, ''A simple higher-order theory for laminated composite plates,'' J. Appl. Mech. ASME **51**, 745–752 (1984).

[3] J. N. Reddy and D. H. Robbins, Jr., ''Theories and computational models for laminated composite laminates,'' Appl. Mech. Rev. **47**(6), 147–169 (1994).

[4] A. K. Noor and W. S. Burton, ''Assessment of shear deformation theories for multilayered composite plates,'' Appl. Mech. Rev. **42**(1), 1–13 (1989).

[5] J. N. Reddy and N. D. Phan, ''Stability and vibration of isotropic, orthotropic and laminated plates according to a higher-order shear deformation theory,'' J. Sound Vib. **98**(2), 157–170 (1985).

[6] Mallikarjuna and T. Kant, ''Free vibration of symmetrically laminated plates using a higher-order theory with finite element technique,'' Int. J. Numer. Methods Eng. **28**, 1875–1889 (1989).

[7] R. Rikards, A. Chate, and A. Korjakin, ''Vibration and damping analysis of laminated composite plates by the finite element method,'' Eng. Comput. **12**(1), 61–74 (1995).

[8] K. M. Liew and C. M. Wang, ''pb-2 Rayleigh-Ritz method for general plate analysis,'' Eng. Struct. **15**(1), 55–60 (1993).

[9] C. W. Lim and K. M. Liew, ''Effects of boundary constraints and thickness variations on the vibratory response of rectangular plates,'' Thin-Walled Struct. **17**(2), 133–159 (1993).

[10] K. M. Liew and C. W. Lim, ''Vibratory characteristics of general laminates, I: symmetric trapezoids,'' J. Sound Vib. **183**(4), 615–642 (1995).

[11] K. M. Liew, Y. Xiang, and S. Kitipornchai, ''Research on thick plate vibration: a literature survey,'' J. Sound Vib. **180**(1), 163–176 (1995).

[12] K. M. Liew, ''Solving the vibration of thick symmetric laminates by Reissner/Midlin plate theory and the p-Ritz method,'' J. Sound Vib. **198**(3), 343–360 (1996).

[13] J. M. Whitney, *Structural Analysis of Laminated Anisotropic Plates* (Technomic, Lancaster, PA, 1987), pp. 39–40.

[14] B. Baharlou and A. W. Leissa, ''Vibration and buckling of generally laminated composite plates with arbitrary edge conditions,'' Int. J. Mech. Sci. **29**(8), 545–555 (1987).

[15] A. W. Leissa, *Vibration of shells* (NASA SP-288) (U.S. Government Printing Office, Washington DC, 1973), p. 43.

[16] R. D. Mindlin, ''Influence of rotary inertia and shear on flexural motions of isotropic, elastic plates,'' J. Appl. Mech. **18**, 31–38 (1951).

[17] A. K. Noor, ''Free vibrations of multilayered composite plates,'' AIAA J. **11**, 1038–1039 (1973).

[18] S. Srinivas and A. K. Rao, ''Bending, vibration and buckling of simply supported thick orthotropic rectangular plates and laminates,'' Int. J. Solids Struct. **6**(8), 1463–1481 (1970).